and overestimated observed GPP and CO_2 amplitude trends with a too-simplistic phenology model that only accounts for temperature effects but ignores radiation and hydrological effects on seasonal leaf development (*26*) (LPJmL-oldPhen in Fig. 3). These examples demonstrate a strong but complex control of climate on plant productivity in northern ecosystems, which ultimately results in the major contribution of enhanced plant growth to the strong CO_2 amplitude trends in northern latitudes.

Our results suggest that a major driver of the large increase in CO_2 amplitude at high northern latitudes involves the interaction of recent climate change with vegetation dynamics. Climate change affects processes such as plant physiology, phenology, water availability, and vegetation dynamics, ultimately leading to increased plant productivity and vegetation cover in northern ecosystems in recent decades. Our results further highlight the gradual replacement of herbaceous vegetation with forests as a major specific factor. Lastly, we identified a dominance of changes in photosynthesis over respiration in driving the changes. Sensitivities of these processes to climate need to be carefully assessed in current ecosystem and Earth system models against observational data to accurately reproduce observed changes in CO_2 amplitude. However, the stimulation of photosynthesis and vegetation growth by climate change cannot be unlimited because of nutrient limitations, radiation, and possibly increased mortality (*32*). Thus, at some point in the future, the positive trends in plant productivity (and thus the CO_2 amplitude increase) might stall. Continued long-term observation of atmospheric CO_2, together with ground and satellite observations of vegetation productivity and dynamics, will be the key to detection, modeling, and better prediction of such changes in high-latitude carbon cycle dynamics.

REFERENCES AND NOTES

1. C. D. Keeling, J. F. S. Chin, T. P. Whorf, *Nature* **382**, 146–149 (1996).
2. J. T. Randerson, M. V. Thompson, T. J. Conway, I. Y. Fung, C. B. Field, *Global Biogeochem. Cycles* **11**, 535–560 (1997).
3. R. B. Bacastow, C. D. Keeling, T. P. Whorf, *J. Geophys. Res.* **90**, 10529–10540 (1985).
4. H. D. Graven *et al.*, *Science* **341**, 1085–1089 (2013).
5. M. Heimann, C. D. Keeling, C. J. Tucker, in *Aspects of Climate Variability in the Pacific and the Western Americas*, D. H. Peterson, Ed. (American Geophysical Union, Washington, DC, 1989), pp. 277–303.
6. IPCC, *Climate Change 2013—The Physical Science Basis: Working Group I Contribution to the Fifth Assessment Report of the Intergovernmental Panel on Climate Change* (Cambridge Univ. Press, 2014).
7. R. B. Myneni, C. D. Keeling, C. J. Tucker, G. Asrar, R. R. Nemani, *Nature* **386**, 698–702 (1997).
8. W. Lucht *et al.*, *Science* **296**, 1687–1689 (2002).
9. I. H. Myers-Smith *et al.*, *Environ. Res. Lett.* **6**, 045509 (2011).
10. L. T. Berner, P. S. A. Beck, A. G. Bunn, S. J. Goetz, *Glob. Change Biol.* **19**, 3449–3462 (2013).
11. P. S. A. Beck *et al.*, *Glob. Change Biol.* **17**, 2853–2866 (2011).
12. M. Jung *et al.*, *J. Geophys. Res.* **116**, G00J07 (2011).
13. A. Anav *et al.*, *Rev. Geophys.* **53**, 785–818 (2015).
14. C. Rödenbeck, S. Houweling, M. Gloor, M. Heimann, *Atmos. Chem. Phys.* **3**, 1919–1964 (2003).
15. J. M. Gray *et al.*, *Nature* **515**, 398–401 (2014).
16. N. Zeng *et al.*, *Nature* **515**, 394–397 (2014).
17. J. Barichivich *et al.*, *Glob. Change Biol.* **19**, 3167–3183 (2013).
18. N. MacBean, P. Peylin, *Nature* **515**, 351–352 (2014).
19. Z. Zhu *et al.*, *Remote Sens.* **5**, 927–948 (2013).
20. S. Sitch *et al.*, *Glob. Change Biol.* **9**, 161–185 (2003).
21. A. Bondeau *et al.*, *Glob. Change Biol.* **13**, 679–706 (2007).
22. M. Heimann, S. Körner, "The global atmospheric tracer model TM3," *Tech. Rep. Max Planck Inst. Biogeochem. 5* (2003), p. 131.
23. See supplementary materials on *Science* Online.
24. S. Schaphoff *et al.*, *Environ. Res. Lett.* **8**, 014026 (2013).
25. K. Thonicke *et al.*, *Biogeosciences* **7**, 1991–2011 (2010).
26. M. Forkel *et al.*, *Biogeosciences* **11**, 7025–7050 (2014).
27. M. Forkel *et al.*, *Glob. Change Biol.* **21**, 3414–3435 (2015).
28. M. Reichstein *et al.*, *Nature* **500**, 287–295 (2013).
29. C. Beer *et al.*, *Science* **329**, 834–838 (2010).
30. R. J. Norby *et al.*, *Proc. Natl. Acad. Sci. U.S.A.* **102**, 18052–18056 (2005).
31. M. Reichstein *et al.*, *Geophys. Res. Lett.* **34**, L01402 (2007).
32. S. Trumbore, P. Brando, H. Hartmann, *Science* **349**, 814–818 (2015).

ACKNOWLEDGMENTS

We thank the following institutions and scientists that acquired and provided CO_2 site data: E. Dlugokencky (NOAA), Scripps Institution of Oceanography, D. Worthy (Environment Canada), F. Meinhardt (Umweltbundesamt), R. Langenfelds and P. Krummel (CSIRO), and H. Koide (JMA). We further thank the following groups, institutions, or scientists for sharing their data sets: AFS, CRU, EC/JRC, ECMWF, GIMMS, NCEP, NRCan, L. Giglio (UMD), M. Jung (MPI-BGC), and S. E. Mikaloff Fletcher (National Institute of Water and Atmospheric Research). We thank S. Schaphoff (PIK) for comments on LPJmL and I. C. Prentice and R. Thomas for comments on the manuscript. Supported by the European Union (FP7) through the projects GEOCARBON (283080), CARBONES (242316), and EMBRACE (283201); U.S. Department of Energy grant DE-SC0012167; NSF grant 1304270; and NOVA grant UID/AMB/04085/2013. Table S7 provides an overview of used data and how it can be obtained. Results from factorial model experiments with LPJmL+TM3 are available at http://doi.pangaea.de/10.1594/PANGAEA.856722.

SUPPLEMENTARY MATERIALS

www.sciencemag.org/content/351/6274/696/suppl/DC1
Materials and Methods
Supplementary Text
Figs. S1 to S13
Tables S1 to S7
References (*33*–*69*)

4 May 2015; accepted 11 January 2016
Published online 21 January 2016
10.1126/science.aac4971

GLOBAL WATER CYCLE

A decade of sea level rise slowed by climate-driven hydrology

J. T. Reager,[1]* A. S. Gardner,[1] J. S. Famiglietti,[1,2] D. N. Wiese,[1] A. Eicker,[3] M.-H. Lo[4]

Climate-driven changes in land water storage and their contributions to sea level rise have been absent from Intergovernmental Panel on Climate Change sea level budgets owing to observational challenges. Recent advances in satellite measurement of time-variable gravity combined with reconciled global glacier loss estimates enable a disaggregation of continental land mass changes and a quantification of this term. We found that between 2002 and 2014, climate variability resulted in an additional 3200 ± 900 gigatons of water being stored on land. This gain partially offset water losses from ice sheets, glaciers, and groundwater pumping, slowing the rate of sea level rise by 0.71 ± 0.20 millimeters per year. These findings highlight the importance of climate-driven changes in hydrology when assigning attribution to decadal changes in sea level.

Over the past century, sea level rose at an average rate of 1.5 ± 0.2 mm year^{-1}, increasing to 3.2 ± 0.4 mm year^{-1} during the past two decades (*1*). The increase in the rate of rise is attributed to an increase in mass loss from glaciers and ice sheets and to ocean warming. Although these contributions are fairly well constrained, trends in sea level also contain a land water storage component that is acknowledged to be among the most important yet most uncertain contributions (*1*–*3*), in which land water storage is defined by the Intergovernmental Panel on Climate Change (IPCC) (*1*) as all snow, surface water, soil moisture, and groundwater storage, excluding glaciers. Every year, land temporarily stores then releases a net 6000 ± 1400 Gt of mass through the seasonal cycling of water, which is equivalent to an oscillation in sea level of 17 ± 4 mm (*4*–*6*). Thus, natural changes in interannual to decadal cycling and storage of water from oceans to land and back can have a large effect on the rate of sea level rise (SLR) on decadal intervals (*7*, *8*). From 2003 to 2011, SLR slowed to a rate of ~2.4 mm year^{-1} (*9*) during a period of increased mass loss from glaciers (*10*) and ice sheets (*11*). Climate-driven changes in land water storage have been suggested to have contributed to this slowdown (*9*), but this assertion has not been verified with direct observations.

Until recently, little data have existed to constrain land water storage contributions to global

[1]Jet Propulsion Laboratory, California Institute of Technology, CA, USA. [2]Department of Earth System Science, Department of Civil and Environmental Engineering, University of California, Irvine, CA, USA. [3]Institute of Geodesy and Geoinformation, University of Bonn, Bonn, Germany. [4]Department of Atmospheric Sciences, National Taiwan University, Taipei, Taiwan.
*Corresponding author. E-mail: john.reager@jpl.nasa.gov

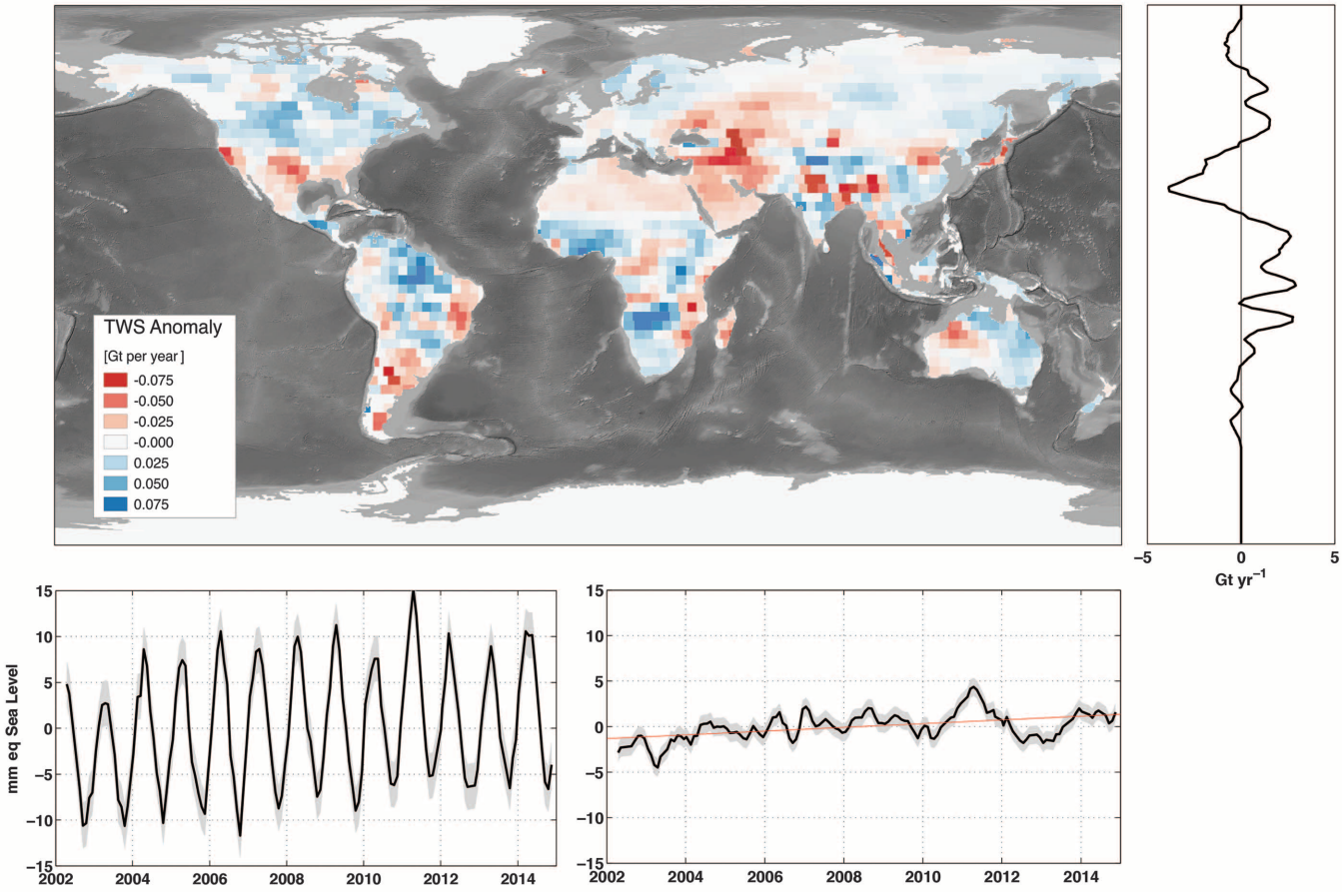

Fig. 1. Trends in land water storage from GRACE observations, April 2002 to November 2014. Glaciers and ice sheets are excluded. Shown are the global map (gigatons per year per 1/2-degree grid), zonal total trends, full time series (millimeters per year SLE), and best-fit linear regression with climatology removed (millimeters per year SLE). The strongest gains and losses are associated with climate-driven variability in precipitation.

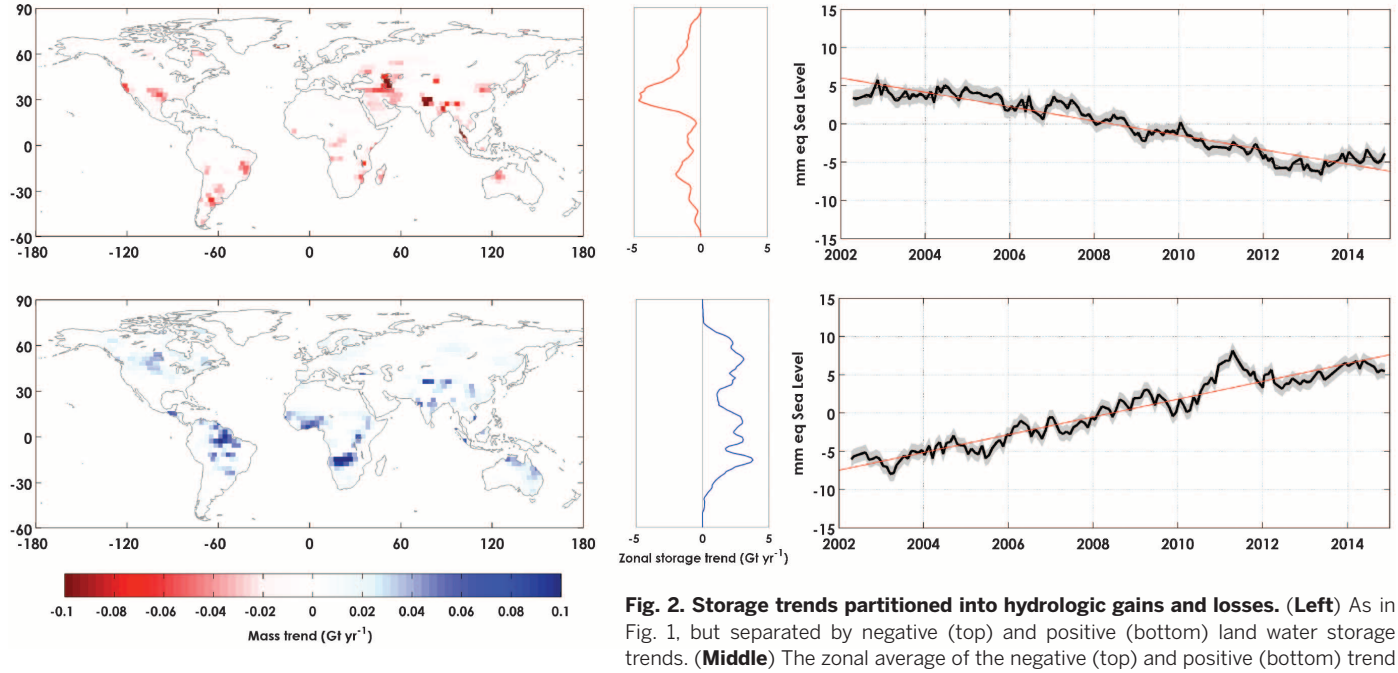

Fig. 2. Storage trends partitioned into hydrologic gains and losses. (**Left**) As in Fig. 1, but separated by negative (top) and positive (bottom) land water storage trends. (**Middle**) The zonal average of the negative (top) and positive (bottom) trend map (gigatons per year per 1/2-degree grid). (**Right**) GRACE land water storage time series averaged for the negative (top) and positive (bottom) land water storage trend map (climatology removed). Estimated glacier trends are shown in the supplementary materials (*44*).

Table 1. Estimates of net direct-human water management contributions to SLR from previous studies. The range of estimates results from different methodological approaches and assumptions, including modeling, remote sensing, and ground-based methods. To achieve a net human-driven contribution, the IPCC AR5 applied an estimate of reservoir retention to the average of the Konikow (*14*) and Wada (*13*) groundwater depletion estimates.

Previous studies	Method	Time period	Contribution (mm year^{-1} SLE)
Konikow *et al.* (2011)	Scaling of in situ measurements	2000 to 2008	0.41 ± 0.10
Wada *et al.* (2012)	PCR-GLB Model	2000	0.57 ± 0.09
Döll *et al.* (2014)	WaterGAP Model	2000 to 2009	0.31 ± 0.0
IPCC AR5 (2013)	(*13*) + (*14*) averaged (including reservoirs)	1993 to 2010	0.38 ± 0.12
Richey *et al.* (2015)	GRACE net subsurface storage	2003 to 2014	0.24 ± 0.02

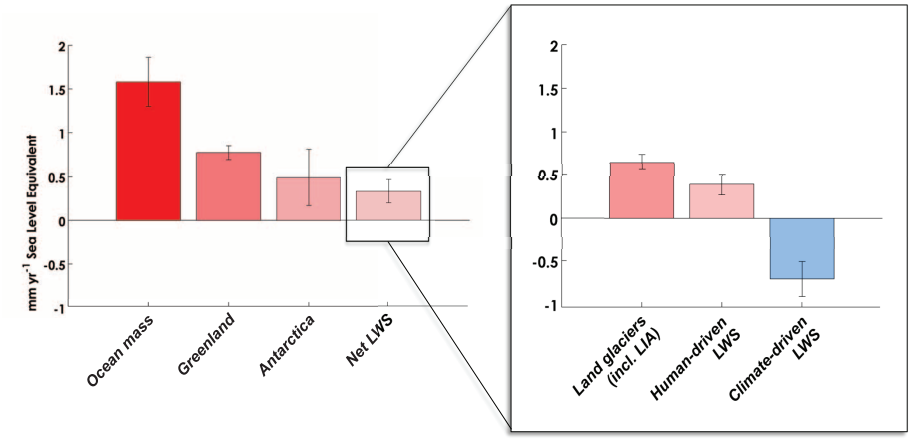

Fig. 3. Observed global mass contributions to SLR, 2002 to 2014, including the disaggregated land water storage term. (**Left**) Global mass contributions to sea level from GRACE mascons, including total ocean mass change (1.58 mm year^{-1} SLE), partitioned between contributions from Greenland (0.77 mm year^{-1} SLE), Antarctica (0.49 mm year^{-1} SLE), and net land water storage (LWS) (0.32 mm year^{-1} SLE). (**Right**) Disaggregation of net LWS contributions, including the estimate of land glacier losses (0.65 mm year^{-1}) anthropogenic hydrology (0.38 mm year^{-1}) (*1*), and climate-driven land water storage from this study (−0.71 mm year^{-1}).

Table 2. The components of total continental water storage used to calculate climate-driven land water storage change from April 2002 to November 2014. LIA, Little Ice Age correction (supplementary materials).

	Source	Contribution (mm year^{-1} SLE)	Uncertainty (mm year^{-1})
Land glaciers (including LIA)	This study	0.65	± 0.09
Human-driven land water storage	IPCC AR5 (*1*)	0.38	± 0.12
Climate-driven land water storage	This study	−0.71	± 0.20
Total continental water storage	This study	0.32	± 0.13

mean SLR. As a result, this term has either been excluded from SLR budgets (*3*) or has been approximated by using ad hoc accounting that includes modeling or scaling of a variety of ground-based observations (*1*, *2*). Human-induced changes in land water storage (hereafter referred to as "human-driven land water storage") include the direct effects of groundwater extraction, irrigation, impoundment in reservoirs, wetland drainage, and deforestation. These activities may play a major role in modulating rates of sea level change (*12*–*16*), and several studies of large aquifers suggest that trends in regional and global land water storage are now strongly influenced by the effects of groundwater withdrawal (*17*). Currently, human activity (including groundwater depletion and reservoir impoundment) is estimated to have directly resulted in a net 0.38 ± 0.12 mm year^{-1} sea level equivalent (SLE) between 1993 and 2010 (*1*) or 15 to 25% of observed barystatic SLR, but estimates are acknowledged to have large uncertainties (*18*–*20*).

Climate-driven variability in rainfall, evaporation, and runoff also contributes to decadal rates of sea level change through changes in the total amount of water held in snow, soil, surface waters, and aquifers (*8*, *21*). Climate-driven changes in land water storage have been assumed to be too small to include in sea level budgets (*1*), but there is little observational evidence to support this assumption. The vast spatial scale of climate-driven changes in land water storage has made them too difficult to observe with accuracy (*22*). As such, current IPCC sea level budgets exclude a potentially large water storage term that is required for closure of barystatic SLR on decadal time scales.

We assessed the role of land water storage in SLR over the 12-year period from 2002 to 2014. We examined global changes in surface mass derived from satellite measurements of time-variable gravity that are well-suited to constrain global changes in water storage. From this data, we extracted an observation-based estimate of the net contributions of the continents to SLR. By incorporating recently reconciled estimates of glacier losses [an update to Gardner *et al.* (*10*)] and recent estimates of global groundwater depletion (*1*, *13*–*16*), we are able to disaggregate this net mass change into the contributions of glaciers, direct human-driven land water storage, and climate-driven land water storage.

Measurements of time-variable gravity come from NASA's Gravity Recovery and Climate Experiment (GRACE) satellite mission (*23*). GRACE provides monthly observations of changes in the Earth's gravity field that, after the removal of signals owing to changes in solid earth and atmosphere, result from the movement of water and ice through the Earth system at specific temporal and spatial scales. GRACE has provided monthly gravity field solutions since April 2002 and has proved to be an effective tool with which to observe changes in the mass of ice sheets (*24*), glaciers (*10*, *25*–*27*), snow mass (*28*), regional groundwater storage (*17*, *29*, *30*), and surface water storage (*31*). Previous studies have shown that because the accuracy of GRACE measurements generally increases with the size of the domain, GRACE observations may be useful to constrain hydrology contributions to sea level change (*6*, *32*–*34*), although only Rietbroek *et al.* (*35*) have attempted to disaggregate those contributions by process. The increasing length of the GRACE record, combined with recent improvements in the processing of the intersatellite range-rate measurements (*36*) and modeling of gravity change resulting from changes in solid earth displacement (supplementary materials, materials and methods) (*37*), have now made the GRACE record more relevant to investigation of land water storage contributions to sea level.

We used 140 monthly solutions from the new Jet Propulsion Laboratory GRACE mascon solution (JPL RL05M) (*36*) for the period spanning April 2002 through November 2014. The JPL RL05M mascon solution solves for gravity anomalies in terms of globally distributed, equal-area 3° spherical cap mass concentration functions coupled with Bayesian regularization based on near-global geophysical models and altimetry observations. This approach optimally reduces correlated error in the gravity solution, resulting in less signal loss and higher spatial resolution than those of traditional methods. The solution also applies a post-processing algorithm to better partition between land and ocean mass changes, limiting "leakage" signal between oceans and land.

Several post-processing corrections are applied to the GRACE solutions in order to correct for known limitations of the GRACE measurements and to isolate the terrestrial water storage signal of interest. These include replacing the degree 2, order 0 spherical harmonic coefficients for each month with those estimated from satellite laser ranging (*38*), correcting the position of the mean pole (*39*), adding an estimate of geocenter motion (*40*), removing a Glacial Isostatic Adjustment (GIA) signal (*37*), removing a glacier change signal (*10*), and removing solid earth response to tectonic events (*41*). Because little to no trend in mass over Greenland and Antarctica is attributed to changes in land water storage, these regions are excluded from our analysis.

The resulting mass anomalies, with appropriately propagated errors, are attributable to changes in land water storage. We estimate a total continental land mass change (including glaciers) over the study period of −0.32 ± 0.13 mm year^{-1} SLE (ocean gaining). To show that our work is consistent with current knowledge, we compared trends in our mascon-based land and ocean mass change time series with mass trends reported by Riva *et al.* (*42*), Llovel *et al.* (*34*), Llovel *et al.* (*43*), and Jensen *et al.* (*6*). In all cases, we find good agreement with earlier works when time periods over which trends are calculated are properly accounted for. We then proceeded to remove glacial signals in order to isolate a hydrology-only "land water storage" signal (*44*).

Shown in Fig. 1 is a global map of the GRACE-observed trend in hydrologic land water storage only (after removing glacier signals) over the 2002–2014 period as well as the global time series; in Fig. 1, blue indicates water gains, and red indicates water losses. Globally, glacier-free land gained water at a rate of 120 ± 60 Gt year^{-1} (0.33 ± 0.16 mm year^{-1} SLE). Regionally, we find good agreement with previous hydrology studies that have applied GRACE to determine water mass trends for individual water basins and aquifers. Positive trends are generally associated with climate variations rather than human water management—such as large flooding periods in the upper Missouri River basin (*45*), recovery from drought in the Amazon (*46*) and the Zambezi and Niger basins in Africa (*47*–*49*), and weaker gains in Northern Australia associated with La Niña (*50*)—and are consistent with observed land precipitation changes during the observation period (*45*). A small portion of the gain signal can also be attributed to human activities—primarily, the filling of reservoirs. Land water storage losses are generally associated with changing precipitation patterns (*45*) and drought, and with human-driven change, primarily attributable to groundwater depletion. The negative trends in land water storage in Fig. 1 correspond well with recent studies of global groundwater stress (*17*) and with regional studies of groundwater depletion in the Middle East region (*51*, *52*), Northwestern India (*29*), California and the Southern High Plains in North America (*30*, *53*, *54*), and the North China Plain (*55*).

To highlight the spatial patterns of change, we partition the global land water storage trend map into its positive and negative components in Fig. 2, left. A spatial mask was constructed at the interface between positive and negative trend signals (along the zero-trend contour) for individual mascons. The partitioned trend maps and their zonal averages (Fig. 1, right, and Fig. 2, center) reveal a distinct pattern of mid-latitude drying, which is more pronounced in the northern hemisphere, and of high- and low-latitude wetting.

We measured a gross negative mass trend of −350 Gt year^{-1}, or −0.97 mm year^{-1} SLE (ocean gaining), for 2002–2014 land water storage losses (Fig. 2, top), which includes human-driven changes in storage, largely due to groundwater depletion as a portion of the total. Recent estimates proposed by IPCC (*1*) for the net human-driven land water storage contribution to sea level (0.38 ± 0.12 mm year^{-1}, 1993–2010) represent only a fraction (<40%) of the total losses observed here, which is expected because our results also include the previously unknown climate-driven land water storage signal. We also measured a gross positive mass trend of 470 Gt year^{-1}, or 1.3 mm year^{-1} SLE for the gaining land water storage regions (Fig. 2, bottom). The combined impacts of gaining and losing regions in land water storage result in a net sea level decrease that can be largely attributable to decadal-scale climate-driven processes.

Our analysis indicates that land water storage acted as a net sea level sink during the 2002–2014 period, resulting from a balance between human- and climate-driven changes in hydrology. Using previously published estimates of the direct anthropogenic component of this balance, we are able to isolate changes in land water storage resulting from climate variability. Recent research on direct human-driven changes in land water storage (*10*–*14*) has yielded a suite of estimates whose mean (−0.38 ± 0.11 mm year^{-1}) is not significantly different than the IPCC (*1*) 1993–2010 estimate of −0.38 ± 0.12 mm year^{-1} SLE (*45*), even though study estimates span a range of temporal intervals (Table 1). Because the net land water storage mass gain calculated here (0.33 ± 0.16 mm year^{-1}) represents the sum of both the human- and climate-driven components of land water storage change, we subtracted the IPPC estimate for human-driven changes to calculate a climate-driven land water storage uptake equivalent to −0.71 ± 0.20 mm year^{-1} SLE. This climate-driven land water storage uptake is required to close the observed land water storage balance (Fig. 3 and Table 2) (*1*). This result is consistent with the hypothesis posed by Cazenave *et al.* (*9*) that El Niño Southern Oscillation (ENSO) modulations of the global water cycle are important in sea level budgeting because they augment the delivery of water to the continents (*19*, *44*). However, we recognize that the hydrologic variability observed here could change with a longer record and may not represent a long-term offset to global SLR.

To illustrate the importance of including climate-driven changes in land water storage in decadal sea level budgets, we place our estimate of climate-driven land water storage uptake in the context of other mass contributions to sea level change as estimated by using the JPL RL05M GRACE mascon solution (*45*), the results of which are shown in Fig. 3. Over the past decade, climate-driven land water storage uptake is of opposite sign and of magnitude comparable with ice losses from glaciers and ice sheets and nearly twice as large as mass losses from direct human-driven changes in land water storage. Our results show that climate-driven changes in land water storage are now observable on a global scale and that these changes are large and necessary for closure of decadal-scale sea level budgets.

REFERENCES AND NOTES

1. J. A. Church *et al.*, in *Climate Change 2013: The Physical Science Basis. Contribution of Working Group I to the Fifth Assessment Report of the Intergovernmental Panel on Climate Change*, T. F. Stocker *et al.*, Eds. (Cambridge Univ. Press, 2013).
2. J. A. Church *et al.*, in *Climate Change 2001: The Physical Scienc Basis. Contribution of Working Group I to the Third Assessment Report of the Intergovernmental Panel on Climate Change*, B.C. Douglas, A. Ramirez, Eds. (Cambridge Univ. Press, 2001).
3. N. L. Bindoff *et al.*, in *Climate Change 2007: The Physical Science Basis. Contribution of Working Group I to the Fourth Assessment Report of the Intergovernmental Panel on Climate Change*, S. Solomon *et al.*, Eds. (Cambridge Univ. Press, 2007).
4. D. P. Chambers, J. Wahr, R. S. Nerem, *Geophys. Res. Lett.* **31**, L13310 (2004).
5. B. Wouters, R. E. M. Riva, D. A. Lavallée, J. L. Bamber, *Geophys. Res. Lett.* **38**, L03303 (2011).
6. L. Jensen, R. Rietbroek, J. Kusche, *J. Geophys. Res. Oceans* **118**, 212–226 (2013).
7. P. C. D. Milly, A. Cazenave, C. Gennero, *Proc. Natl. Acad. Sci. U.S.A.* **100**, 13158–13161 (2003).
8. T. H. Syed, J. S. Famiglietti, D. P. Chambers, J. K. Willis, K. Hilburn, *Proc. Natl. Acad. Sci. U.S.A.* **107**, 17916–17921 (2008).
9. A. Cazenave *et al.*, *Nature Climate Change* **4**, 358–361 (2014).
10. A. S. Gardner *et al.*, *Science* **340**, 852–857 (2013).
11. A. Shepherd *et al.*, *Science* **338**, 1183–1189 (2012).
12. B. F. Chao, Y. H. Wu, Y. S. Li, *Science* **320**, 212–214 (2008).
13. Y. Wada *et al.*, *Geophys. Res. Lett.* **39**, L09402 (2012).
14. L. F. Konikow, *Geophys. Res. Lett.* **38**, L17401 (2011).
15. Y. N. Pokhrel *et al.*, *Nat. Geosci.* **5**, 389–392 (2012).
16. P. Döll, H. Müller Schmied, C. Schuh, F. T. Portmann, A. Eicker, *Water Resour. Res.* **50**, 5698–5720 (2014).
17. A. S. Richey *et al.*, *Water Resour. Res.* **51**, 5217–5238 (2015).
18. J. Gonçalvès, J. Petersen, P. Deschamps, B. Hamelin, O. Baba-Sy, *Geophys. Res. Lett.* **40**, 2673–2678 (2013).
19. M.-H. Lo, J. S. Famiglietti, *Geophys. Res. Lett.* **40**, 301–306 (2013).
20. L. F. Konikow, *Nat. Geosci.* **6**, 2 (2013).
21. C. Boening, J. K. Willis, F. W. Landerer, R. S. Nerem, J. Fasullo, *Geophys. Res. Lett.* **39**, L19602 (2012).
22. D. Lettenmaier, P. Milly, *Nat. Geosci.* **2**, 452–454 (2009).

23. B. D. Tapley, S. Bettadpur, J. C. Ries, P. F. Thompson, M. M. Watkins, *Science* **305**, 503–505 (2004).
24. I. Velicogna, J. Wahr, *Science* **311**, 1754–1756 (2006).
25. S. B. Luthcke, A. A. Arendt, D. D. Rowlands, J. J. McCarthy, C. F. Larsen, *J. Glaciol.* **54**, 767–777 (2008).
26. A. S. Gardner *et al.*, *Nature* **473**, 357–360 (2011).
27. T. Jacob, J. Wahr, W. T. Pfeffer, S. Swenson, *Nature* **482**, 514–518 (2012).
28. G.-Y. Niu *et al.*, *Geophys. Res. Lett.* **34**, L15704 (2009).
29. M. Rodell, I. Velicogna, J. S. Famiglietti, *Nature* **460**, 999–1002 (2009).
30. J. S. Famiglietti *et al.*, *Geophys. Res. Lett.* **38**, L03403 (2011).
31. H. Kim, P. J.-F. Yeh, T. Oki, S. Kanae, *Geophys. Res. Lett.* **36**, L17402 (2009).
32. G. Ramillien *et al.*, *Global Planet. Change* **60**, 381–392 (2008).
33. P. C. D. Milly *et al.*, in *Understanding Sea-Level Rise and Variability*, J. A. Church, P. L. Woodworth, T. Aarup, W. S. Wilson, Eds. (Wiley-Blackwell, 2010), pp. 226–255.
34. W. Llovel, M. Becker, A. Cazenave, J.-F. Crétaux, G. Ramillien, *C. R. Geosci.* **342**, 179–188 (2010).
35. R. Rietbroek, S.-E. Brunnabend, J. Kusche, J. Schroeter, C. Dahle, *Proc. Natl. Acad. Sci. U.S.A.* 10.1073/pnas.1519132113 (2015).
36. M. M. Watkins, D. N. Wiese, D.-N. Yuan, C. Boening, F. W. Landerer, *J. Geophys. Res. Solid Earth* **120**, 2648–2671 (2015).
37. W. R. Peltier, D. F. Argus, R. Drummond, *J. Geophys. Res. Solid Earth* **120**, 450–487 (2015).
38. M. Cheng, B. D. Tapley, *J. Geophys. Res.* **109** (B9), B09402 (2004).
39. J. Wahr, R. S. Nerem, S. V. Bettadpur, *J. Geophys. Res. Solid Earth* **120**, 4597–4615 (2015).
40. S. Swenson, D. Chambers, J. Wahr, *J. Geophys. Res.* **113** (B8), B08410 (2008).
41. S.-C. Han, R. Riva, J. Sauber, E. Okal, *J. Geophys. Res. Solid Earth* **118**, 1240–1267 (2013).
42. R. Riva, J. Bamber, D. Lavallee, B. Wouters, *Geophys. Res. Lett.* **37**, L19605 (2010).
43. W. Llovel, J. K. Willis, F. W. Landerer, I. Fukumori, *Nature Climate Change* **4**, 1031–1035 (2014).
44. Materials and methods are available as supplementary materials on *Science* Online.
45. J. T. Reager, B. F. Thomas, J. S. Famiglietti, *Nat. Geosci.* **7**, 588–592 (2014).
46. J. L. Chen, C. R. Wilson, B. D. Tapley, *Water Resour. Res.* **46**, W12526 (2010).
47. G. Ramillien, F. Frappart, L. Seoane, *Remote Sens.* **6**, 7379–7405 (2014).
48. E. Forootan *et al.*, *Surv. Geophys.* **35**, 913–940 (2014).
49. J. T. Reager, J. S. Famiglietti, *Geophys. Res. Lett.* **36**, L23402 (2009).
50. J. T. Fasullo, C. Boening, F. W. Landerer, R. S. Nerem, *Geophys. Res. Lett.* **40**, 4368–4373 (2013).
51. K. A. Voss *et al.*, *Water Resour. Res.* **49**, 904–914 (2013).
52. E. Forootan *et al.*, *Remote Sens. Environ.* **140**, 580–595 (2014).
53. B. R. Scanlon, L. Longuevergne, D. Long, *Water Resour. Res.* **48**, W04520 (2012).
54. B. R. Scanlon *et al.*, *Proc. Natl. Acad. Sci. U.S.A.* **109**, 9320–9325 (2012).
55. W. Feng *et al.*, *Water Resour. Res.* **49**, 2110–2118 (2013).

ACKNOWLEDGMENTS

We thank M. Watkins, E. Ivins, D. Argus, G. Cogley, A. Richey, Y. Wada, R. Nerem, and D. Chambers for their contributions and discussion. This work was supported by funding from the NASA NEWS, Sea Level, and Cryosphere programs; the NASA GRACE Science Team; and the University of California Multicampus Research Programs and Initiatives. This multidisciplinary collaboration grew from the interactions of the NASA Sea Level Change Team. The research was conducted at the University of California, Irvine and at the Jet Propulsion Laboratory, California Institute of Technology under contract with NASA. M.-H. Lo was supported by the Ministry of Science and Technology (MOST), Taiwan, MOST 103-2111-M-002-006. GRACE RL05M data are available at podaac.jpl.nasa.gov. The authors declare no competing interests.

SUPPLEMENTARY MATERIALS

www.sciencemag.org/content/351/6274/699/suppl/DC1
Materials and Methods
Figs. S1 to S11
Tables S1 to S4
References (*56*–*69*)

9 November 2015; accepted 7 January 2016
10.1126/science.aad8386

MICROBIAL PHYSIOLOGY

Artificial electron acceptors decouple archaeal methane oxidation from sulfate reduction

Silvan Scheller,* Hang Yu, Grayson L. Chadwick, Shawn E. McGlynn,† Victoria J. Orphan*

The oxidation of methane with sulfate is an important microbial metabolism in the global carbon cycle. In marine methane seeps, this process is mediated by consortia of anaerobic methanotrophic archaea (ANME) that live in syntrophy with sulfate-reducing bacteria (SRB). The underlying interdependencies within this uncultured symbiotic partnership are poorly understood. We used a combination of rate measurements and single-cell stable isotope probing to demonstrate that ANME in deep-sea sediments can be catabolically and anabolically decoupled from their syntrophic SRB partners using soluble artificial oxidants. The ANME still sustain high rates of methane oxidation in the absence of sulfate as the terminal oxidant, lending support to the hypothesis that interspecies extracellular electron transfer is the syntrophic mechanism for the anaerobic oxidation of methane.

Biological methane oxidation in the absence of oxygen is restricted to anaerobic methanotrophic archaea (ANME) that are phylogenetically related to methanogens (*1*, *2*). These organisms evolved to metabolize methane to CO_2 near thermodynamic equilibrium ($E^{o\prime}$ = −245 mV for CH_4/CO_2) via the pathway of reverse methanogenesis (*3*), which includes the chemically challenging step of methane activation without oxygen-derived radicals (*4*). Reported terminal electron acceptors for anaerobic oxidation of methane (AOM) include sulfate (*1*, *2*), nitrate (*5*), and metal oxides (*6*). Nitrate reduction coupled to methane oxidation is directly mediated by a freshwater archaeal methanotroph "*Ca. Methanoperedens nitroreducens*" ANME-2d (*5*); however, the electron transport mechanism coupling methane oxidation with other terminal electron acceptors (such as sulfate and metal oxides) is still debated (*7*–*9*).

Sulfate-coupled methane oxidation (Eq. 1) is the dominant mechanism for methane removal within marine sediments, preventing the release of teragrams per year of this greenhouse gas from the oceans (*10*).

$$CH_4 + SO_4^{2-} = HCO_3^- + HS^- + H_2O$$
$$\text{Gibbs free energy } (\Delta G^{o\prime}) = -17 \text{ kJ mol}^{-1} \quad (1)$$

Multiple methanotrophic archaeal lineages (ANME-1; ANME-2a,b,c; and ANME-3) form syntrophic consortia with sulfate-reducing deltaproteobacteria (SRB) that drive AOM in areas of methane release at the seabed (*11*). The metabolism of AOM with sulfate appears to be partitioned between the two partners, requiring the exchange of electrons or intermediates. The mechanism underlying this syntrophic association has been studied using microcosm experiments [with AOM microorganisms exhibiting doubling times of 2 to 7 months (*12*–*17*)], as well as through the application of stable isotope analyses (*2*), radiotracer rate measurements (*18*), metagenomics (*3*, *5*, *19*, *20*), and theoretical modeling (*21*, *22*).

Attempts to metabolically decouple the syntrophic association and identify the intermediate compound passaged between ANME archaea and their SRB partners have been unsuccessful when diffusive intermediates such as hydrogen, acetate, formate, and some redox active organic electron shuttles were used (*16*, *23*). Culture-independent evidence for direct interspecies electron transfer in sulfate-coupled AOM by members of the ANME and their SRB partners (*8*, *9*) supports earlier genomic predictions of this process occurring in the methanotrophic ANME-1 (*19*).

Guided by the recent evidence of direct interspecies electron transfer from ANME-2 to SRB (*8*), we probed whether artificial electron acceptors can substitute for the role of the SRB partner as a terminal oxidant for AOM. Respiration of the artificial electron acceptor 9,10-anthraquinone-2,6-disulfonate (AQDS, $E^{o\prime}$ = −186 mV) has been previously reported in methanogens (*24*). We tested AQDS as a sink for methane-derived electrons generated by the ANME archaea in incubations with deep-sea methane seep sediment. The stoichiometry of methane oxidation coupled to AQDS predicts the reduction of four equivalents of AQDS per methane (Eq. 2).

$$CH_4 + 4\,AQDS + 3H_2O = HCO_3^- + H^+ + 4\,AQH_2DS$$
$$\Delta G^{o\prime} = -41 \text{ kJ mol}^{-1} \quad (2)$$

To quantify AOM with AQDS, we performed anaerobic microcosm experiments using methane seep sediment from the Santa Monica basin

Division of Geological and Planetary Sciences, California Institute of Technology, Pasadena, CA 91125, USA.
***Corresponding author. E-mail: vorphan@gps.caltech.edu (V.J.O.); scheller@caltech.edu (S.S.)** †Present address: Department of Biological Sciences, Tokyo Metropolitan University, Tokyo 192-0397, Japan; and Biofunctional Catalyst Research Team, RIKEN Center for Sustainable Resource Science, Saitama 351-0198, Japan.

A decade of sea level rise slowed by climate-driven hydrology
J. T. Reager, A. S. Gardner, J. S. Famiglietti, D. N. Wiese, A. Eicker and M.-H. Lo (February 11, 2016)
Science **351** (6274), 699-703. [doi: 10.1126/science.aad8386]

Editor's Summary

By land or by sea

How much of an effect does terrestrial groundwater storage have on sea-level rise? Reager *et al.* used gravity measurements made between 2002 and 2014 by NASA's Gravity Recovery And Climate Experiment (GRACE) satellites to quantify variations in groundwater storage. Combining those data with estimates of mass loss by glaciers revealed groundwater's impact on sea-level change. Net groundwater storage has been increasing, and the greatest regional changes, both positive and negative, are associated with climate-driven variability in precipitation. Thus, groundwater storage has slowed the rate of recent sea-level rise by roughly 15%.

Science, this issue p. 699